Atom Indonesia

Journal homepage: http://aij.batan.go.id

# The Investigation of Lead Borate Glass Composites for Boron Neutron Capture Therapy Shielding

**M. S. Ali[1,3], A. M. Abdelmonem[2*], S. K. Elshamndy[2], G. M. Shoraiet[3], T. M. Mustafa[3], G. S. Hassan[4]**

[1]*African Institute for Mathematical Sciences, B. P. 1418 Mbour, Thies Region, Senegal*
[2]*University of Jouf, Faculty of Science and Art, Department of Physics, Post Office 207, Al-Jouf, KSA*
[3]*Physics Department, Faculty of Science, New Valley University, Egypt*
[4]*Physics Department, Faculty of Science, Assiut University, Egypt*

**ARTICLE INFO**

*Article history:*
Received 14 May 2021
Received in revised form 5 January 2022
Accepted 10 April 2022

*Keywords:*
BNCT
Thermal neutron shielding
Gamma-ray shielding
Lead borate glass
Monte carlo simulation

**ABSTRACT**

In this work, we studied the lead borate glass composites to optimize their shielding properties of thermal neutrons and gamma-rays for Boron Neutron Capture Therapy (BNCT) applications. Attenuation coefficients, half-value layer (HVL), and tenth-value layer (TVL) were measured for a broad range of gamma-ray energies, i.e., 356, 511, 662, 1173, 1274, and 1332 keV experimentally. Theoretical results using XCOM software show an agreement with the NaI(Tl) detector-based experimental measurements. The attenuation of collimated thermal neutrons, from the Cf-252 source, was simulated using Monte Carlo-based code and compared experimentally with measurements by $BF_3$ detector. A reasonable agreement between simulations and experiments was observed, suggesting that the shielding properties of lead borate glass (LBG) composites are monotonically increasing with the increase of the lead and boron additives.



## INTRODUCTION

Recently, there is an observed increase in the cancer burden day by day. This inclination has motivated oncology, biochemistry, and medical physics scientists to develop new promising treatments associated with high selectivity that reduce the undesirable dose for normal cells. The current mainstream treatment modalities used to overcome this dangerous burden are surgery, chemotherapy, and radiotherapy [1].

Although these techniques achieve sophisticated progress in fighting cancer spread, all of these therapies encounter essential limitations that need to be investigated and solved, such as the bad side effects associated with each type. Our approach is restricted to solving one of these bad side effects that are related to radiotherapy in general and boron neutron capture therapy in particular.

Boron neutron capture therapy (BNCT) is one of indirect radiation utilization that relies upon using gamma rays emitted from boron neutron capture interaction to damage the tumor at the molecular scale. It is a promising radiotherapy technique that featured high selectivity with regard to the reduction of the destruction to the healthy tissue neighboring the cancer cells, particularly in deep-seated brain tumors, and to exterminate remaining cancer cells after surgical therapy safely [1].

The physics of BNCT depends on using the non-radioactive isotope B-10 atom to absorb low energy, approximately less than 0.5 eV, for the incident thermal neutron beam to produce an alpha particle and the recoiled lithium-7 nucleus. The associated resultant linear energy transfer of alpha particle is significantly high, 150 KeV/micrometer, while it is for Lithium-7 a 175 KeV/micrometer. Besides, a low amount of gamma-ray released could be neglected [2-4].

BNCT technique is considered one of the high selectivity therapies for deep-seated cancers due to the path lengths of the reaction products, which are in the range of 4.5 to 10 micrometers in water or in living tissues. From this perspective, the resultant

* Corresponding author.
E-mail address: amm@ju.edu.sa
DOI: https://doi.org/10.17146/aij.2022.1147

energy deposition is limited to the diameter of the single cell. Depending on the high propensity of the tumor cell for absorbing the boron-10 compounds, this technique is simultaneously capable of sparing the normal cells undesired dose [4] .

Many types of BNCT facilities differ depending on the implemented neutron source or the used beam shaping assembly system. Plentiful types of neutron sources are used in research, industry, and clinical applications, some of them are fixed or portable. For instance, the famous types of BNCT facilities are reactor-based BNCT, accelerator-based BNCT (ABNCT), and Neutron-generators based BNCT such as D-D or D-T based BNCT [4,5].

In fact, enhancing the clinical implementation of BNCT relies upon developing many factors such as dose planning, neutron beam shaping assembly, and shielding systems. Our approach in this manuscript is restricted to optimizing the shielding materials by which adequate radiation protection for the BNCT based clinical facilities can be provided.

Radiotherapy clinical facilities, in general, and BNCT-based, in particular, require shielding systems with special features, which provide highly appropriate radiation protection as well as visibility through the shielding materials. Added to that, choosing the most common commercial materials owing to these features is important to reduce the treatment cost on patients [6].

Glass is considered to be one of the suitable choices to fulfill the double functions required in radiotherapy shielding materials. Intuitively, glazed materials are commercial and easy to fabricate with excellent transparency to be used as optical windows for the operation and maintenance of nuclear facilities in various applications, especially in radiotherapy [7].

It is worth to be mentioned, heavy elements, for instance, lead or tungsten are considered to be appropriate materials for shielding against gamma-ray. Thus, these materials are taken into account to be a convenient additive to other materials, particularly glazed materials to fabricate optical windows for nuclear facilities or to be the inner layer of the shielding system [7].

Besides, both lead and lead-glazed materials are favored over other choices for shielding against gamma-rays and neutrons due to their high densities and atomic numbers (Z) [8]. It is commonly known, the high Z numbers exhibit large cross-sections regarding gamma-ray interactions, and also the density of the shielding materials plays a crucial role in neutron interactions [9].

In fact, the glazed materials involving low atomic numbers, such as H, Li, B, C, etc., recently exhibit suitable performance as shielding materials with regard to neutron radiation, particularly in nuclear reactors and accelerators based nuclear facilities. For instance, it was observed that the gamma particle in nuclear reactors possess energy in the range of 0.10 to 10 MeV while the associated neutron energy spectrum is found to be from 0.18 to 12 MeV with average energy per neutron in the range of 1 to 2 MeV through uranium fission. In recent reactors-based shielding systems, glazed materials containing boron are found to be an appropriate candidate for neutron shielding [10].

From this perspective, lead borate glass composites might be considered to possess extremely valuable in numerous nuclear implementations such as in isotope production, nuclear reactors, accelerator-based applications, diagnostic/imaging rooms, and radiotherapy facilities. This motivated us to investigate the capability of lead borate glazed composites as shielding materials for boron neutron capture therapy as a type of radiotherapy modality.

According to the nature of the radiotherapy application that we were concerned about in this study, our approach was restricted to the investigation of the capability of lead borate glazed composites as shielding materials against gamma-rays and thermal neutron beams. Although the spatial fluxes and angular-based energy distributions of both gamma-rays and thermal neutrons could be calculated theoretically or experimentally for any arbitrary material depending on the associated cross-sections of these particles, the properties of the associated bulk attenuation of the potential candidate materials regarding these two types of particles still required more accurate investigations for shielding analysis and building radiotherapy facilities [11,12].

Added to the previously mentioned story, a vital item that ignites our enthusiasm to investigate the capability of lead borate composites as shielding materials for BNCT-based radiotherapies is the high absorption cross-section of boron against thermal neutrons without releasing high-energy gamma-rays. Consequently, this reason makes the lead borate glazed composites the optimal candidates for BNCT facilities shielding.

In fact, there are plentiful studies focused on investigating the attenuation properties of various elements, mixtures, and compounds against many different radiation particles in a broad range of energy for numerous applications in such a field. Despite these studies, the yielded results are still not sufficient, particularly when these results affect the optimization processes that deal directly with human health.

From this standpoint of view, the role of theorists comes to establish new theoretical platforms by which the attenuation properties could be made predictable. This also motivated us to develop a new program based on the Monte Carlo method to simulate the thermal neutron transport phenomena. This program will be named the Monte Carlo Calculator of Neutronic Attenuation Properties (MCCNAP). The yielded results of this proposed program will be compared with the results of the performed experiments.

Depending on the observed agreements between the simulated predictions and experimental results, the usage of this theoretical platform might be extended to involve other investigations related to optimizing BNCT systems, such as neutron-flux shifters and gamma filters in next future research.

In this work, investigating the endorsement between the theoretical and experimental results of thermal neutron attenuations through various composites of lead borate glazed samples with different densities, varying from 3.95 to 4.41 g/cm$^3$, will be performed statistically using the $\chi^2$ function statistical test. It is worth to be mentioned, the statistical function is defined via Eq. (1):

$$\chi^2 = \frac{1}{n}\sum_{i=1}^{n}\frac{(M_i^{exp}-M_i^{theo})^2}{\Delta_i} \quad (1)$$

The summation in the preceding expression runs over selected results of a particular attenuation property, for instance, thermal neutron attenuation results by which $M_i^{exp}$ refers to the observed thermal neutron counts per second of a specific composite, while $M_i^{theo}$ are the corresponding theoretical results depending on the composite properties such as the density, thickness of the sample, and the total cross-section. Additionally, the $\Delta i$ quantity points to the predictions of the corresponding composites associated with the uncertainty. Finally, n refers to the number of samples under investigation.

The optimization of the reliability of this simulation relies on minimizing the values of this statistical function. The results of the optimization, in terms of the previously mentioned comparison, will be calculated statistically and illustrated in the results and discussion section.

Through this work, the attenuation properties of lead borate glazed composites against gamma-rays were calculated also in both theoretical and experimental manners to evaluate the capability and effectiveness of our proposed composites in shielding. The measured experimental results were performed through the NaI(Tl) scintillation detector, while the theoretical results were calculated theoretically via the XCOM software. Profiles, the theoretical and the experimental, of each sample were compared and represented as well in the result and discussion section.

In the next section, the theoretical background that governs the interactions between the radiation particles, under study, and the matter will be discussed in brief. After that, the used methodology in both schemes, the theoretical and experimental, will be illustrated in the materials and methods section.

## THEORETICAL BACKGROUND AND COMPUTATIONAL WORK

Many attempts are performed to simulate or model mathematically the interactions between the numerous types of radiation and matter for several applications, particularly when the application involves using neutrons. Dealing with neutronic interactions mathematically exhibits some complexity by which the theoretical schemes depend on using random-events numerical schemes, such as the Monte Carlo method, which have been considered to be optimal theoretical recipes to stimulate the neutronic transport phenomena. Consequently, the next section will discuss the nature of both types of radiation with regard to our study and introduce the theoretical methods used to investigate the capability of LBG composites for shielding against these two types.

### Neutron interactions

Generally, neutron particles may undergo specific types of interactions with matter, such as scattering, absorption, and finally fission. The probability of occurring one or more of these interactions relies upon the corresponding microscopic cross-section of the matter for each type of interaction. The sum of these microscopic cross-sections is the total microscopic cross-section.

In the BNCT field of research, studies on the scattering interactions possess a high priority due to their applications in such a field. Consequently, it is important to find potential candidates materials for neutron shielding and also thermalization of high-energy fast neutrons to the required neutron energy for the neutron-capture interactions. According to the associated energy, neutrons interact with matter by inelastic and elastic scattering. For shielding studies, the attenuation processes depend mainly on collisions. The energy transferred by neutrons per collision relies on the nucleons inside the nucleus.

The probabilities of the previously mentioned possible interactions of neutrons with

matter are denoted by $\sigma_S$, $\sigma_a$, and $\sigma_f$ respectively. The sum of these corresponding microscopic cross-sections for each type of neutron interaction is named the total microscopic cross-section, which is denoted by $\sigma_t$ [13].

Actually, the attenuation processes of the neutron beam during its passage via the shielding materials depend not only upon the microscopic cross-sections but also on the number of nuclei inside the medium of the interactions. This concept is related to the density of matter and also the atomic weight. All of these physical quantities are bounded together in a mathematical expression that refers to what we called the total macroscopic cross-section, $\Sigma_t$, which is in $cm^{-1}$ unit [14]. It is obtained according to the following formula in Eq. (2):

$$\Sigma_t = \frac{\rho N_a \sigma_t}{A} \quad (2)$$

where ρ is the density in the unit of g.cm-3, Na is Avogadro's number, and A is the atomic weight.

All of these fundamentals have been considered in our simulation program. Our computational approach relies upon the ingredients of the Monte Carlo method to validate our theoretical platform to perform simulations for various thermalization experiments in regard to not only neutron shielding but also other purposes like thermal-neutron filters. It is usually a very simple and well-characterized experiment in order to make it simple to simulate and reduce the sources of experimental error.

Some assumptions have been considered in our simulation for simplicity, such as that all parts of the materials under investigation are at the same temperature. All generated histories/events start to form the origin point. The initial number of events/neutrons is the detected experimental counts per second at zero thickness of the samples. The reflector boundary conditions are essentially considered in our simulation to avoid losing histories.

Besides, tallies in our simulation are constructed to track the path of the thermal neutrons among a specific thickness of the material under study. Consequently, attenuation calculations are performed using tallies to find the total flux passed through per thickness for each proposed composite.

### Gamma-ray interactions

It is commonly known that the transmission of gamma-ray through any arbitrary material obeys Lambert-Beer's law as Eq. (3):

$$I = I_o e^{-\mu x} \quad (3)$$

According to this law, the transmission phenomenon relies upon the medium thickness x and the associated linear attenuation coefficient, μ, while Io and I are the incidents and the transmitted intensities of the photon beam. It is worth to be mentioned that the value of μ is considered as a parameter that is subject to the features of the matter such as the absorber density and its atomic number. Besides, the value of this parameter depends upon the energy of the associated incident photon.

For shielding purposes, the mass attenuation coefficient is essential to be investigated. It is derived from the previously mentioned expression as Eq. (4):

$$\frac{\mu}{\rho} = \frac{\ln(I_o/I)}{\rho x} \quad (4)$$

where $\mu/\rho$ is the mass attenuation coefficient, and ρ is the density of the shielding medium. Through this work, the associated errors of the mass attenuation coefficient values were evaluated experimentally from the errors in samples' intensities, thicknesses, and mass-densities according to this expression Eq. (5):

$$\Delta(\mu/\rho) = \left(\frac{1}{\rho * x}\right) * \left[\left(\Delta I_o/I_o\right)^2 + \left(\Delta I/I\right)^2 + \left[\ln\left(I_0/I\right)\right]^2 * \left[\left(\Delta\rho/\rho\right)^2 + \left(\Delta x/x\right)^2\right]^{1/2}. \quad (5)$$

Additionally, the calculations through this manuscript involve studying the half-value layer (HVL) and the tenth-value layer (TVL) for each composite under investigation in both manners, theoretically and experimentally. The calculations of HVL and TVL are obtained using these formulas: HVL=0.6932/μ and TVL=2.303/μ, respectively. As mentioned previously, all theoretical calculations associated with gamma-ray investigations were performed via the XCOM software.

## MATERIALS AND EXPERIMENTAL METHODS

### Sample's preparation

Melt-quenching techniques were considered through the preparation stage of lead borate glazed samples [15]. By using these techniques, oxides mixtures were prepared initially to be included in a porcelain crucible. Then, these mixtures were heated to 900 $^oC$ at a rate of 250 $^oC$/hr using an electric furnace. Consequently, each sample was exposed to increasing the heating temperature to reach 1300 $^oC$ for one hour.

Stirring was carefully implemented using a rod of quartz to remove the bubbles from the melted

mixture to ensure homogeneity. Thus, the mixture was poured into a cylindrical mold from stainless steel to be held at room temperature. Afterward, each prepared sample was subjected to an annealing stage using another furnace at 300 $^{o}$C for 12 hours before a gradual cooling at 500 $^{o}$C per hour rate till room temperature.

Each sample of lead borate glazed composites contained various percentages of both lead and boric to be configured in a cylindrical shape that has a 3 cm diameter and 0.4 cm thickness. The considerations of each sample are displayed in Table 1. Ultimately, Archimedes's method was applied to evaluate the corresponding density to each sample as shown in Eq. (6):

$$\rho = \left[\frac{a}{a-b}\right] * 0.86 \quad (6)$$

where (a) is the measured weight of the sample in air, b is the gauged weight in the benzene, and finally, 0.86 is the evaluated density of benzene at 20 $^{o}$C. X-ray diffraction (XRD) investigations were performed for each sample of LBG composites to ensure the absence of crystallization. This test relies upon the lack of the peak in the yielded XRD results, which indicates that all LBG samples are prepared to be amorphous. The XRD spectra of powder LBG samples are illustrated in Fig. 1.

**Table 1.** The elemental compositions for all LBG samples.

| Oxide % | LBG # 1 | LBG # 2 | LBG # 3 | LBG # 4 | LBG # 5 |
|---|---|---|---|---|---|
| B2O3 | 25 | 20 | 15 | 10 | 10 |
| Na2O | 10 | 10 | 10 | 10 | 10 |
| Al2O3 | 2 | 2 | 2 | 2 | 2 |
| SiO2 | 7 | 7 | 7 | 7 | 15 |
| CaO | 3 | 3 | 3 | 3 | 3 |
| PbO | 50 | 55 | 60 | 65 | 55 |
| Bi2O3 | 3 | 3 | 3 | 3 | 3 |
| Total | 100 | 100 | 100 | 100 | 100 |

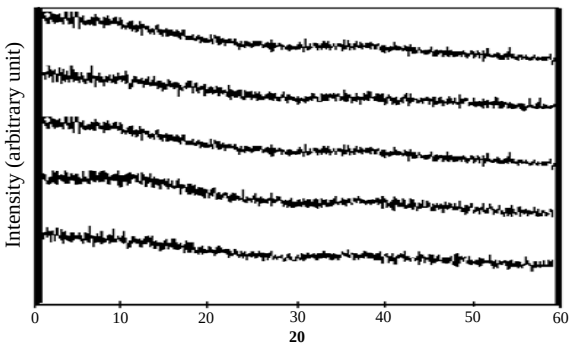


**Fig. 1.** The absence of the peak in XRD spectra emphasizes that all LBG samples are in non-crystalline form.

## Transmission measurements for thermal neutrons

Transmission measurements of thermal neutrons were executed through all composites of LBG using a collimated narrow beam emitted by Cf-252 as a neutron source associated with a rectangular-shaped slit with 0.4 cm x 0.6 cm dimensions. It is worth to be mentioned that using collimated narrow beams for neutron transmission experiments increases the probability to obtain a narrow neutron beam with specific intensity and geometry to optimize the measurement process and also to decrease the side scatters that might affect the results. Through our experiments, a special collimator was used to eliminate the undesired effects of side scatters.

The arrangement of our experimental layout was described somewhere else [16] and is portrayed in Fig. 2. The detection process in our experiments was performed by using $BF_3$ detector electronic chains and its schematic diagram is displayed through Fig. 3.

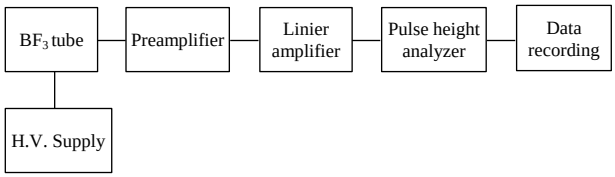


**Fig. 2.** The block diagram of $BF_3$ detector electronic chain.

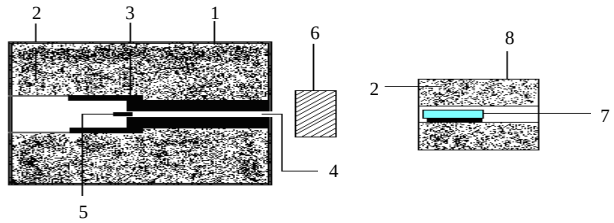


**Fig. 3.** The schematic diagram of the experimental set up using $BF_3$ Detector in which numbers 1 to 8 refers to source collimator, high-density borated paraffin wax, lead shield, neutron beam, Cf-252 neutron source, the sample under investigation, $BF_3$ detector, and detector shield respectively.

## Transmission measurements of gamma-ray

The layout of the gamma transmission experiments is illustrated in Fig. 4. Through these experimental arrangements, the attenuation characteristics of lead borate glazed samples were studied against gamma-ray, which includes a lead housing, a beam collimator that possesses a 0.3 cm inner diameter, and a NaI(Tl) detector in shielding lead. This type of detector is conjugate to a

photomultiplier tube that is settled to a tube involving a dynode chain of the photomultiplier tube. The measurements of the corresponding linear attenuation coefficients of each sample were performed using a 1.5" x 1.5" NaI(Tl) detector, which owns an 8.5 % resolution; full width at half of the maximum, at gamma associated energy, equals 662 keV. Actually, appropriate lead shielding was supplied to both the detector and the source. The electronic block diagram of the NaI(Tl) gamma-ray spectrometer is presented in Fig. 4.

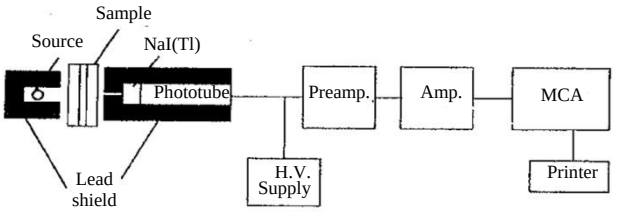


**Fig. 4.** The electronic block diagram of the NaI(Tl) gamma-ray spectrometer.

Besides, the linearity and performance associated with the spectrometer and the experimental setup were examined using the measurement of the linear attenuation coefficient of two slabs of aluminum and lead with thicknesses of 1 cm and 2 mm. The experimental yielded results were compared to these theoretical results predicted by using the XCOM platform. Favored agreements were found, which emphasize the reliability of the used experimental setup and the spectrometer.

## RESULTS AND DISCUSSION

Through this section, the yielded results of the attenuation using lead borate glazed samples, with various thicknesses and different concentrations of elemental composites as displayed in Table 1, against collimated neutron beams from Cf-252 and gamma rays with 356, 511, 662, 1173,1274, and 1332 keV energies will be illustrated and discussed in details. The attenuation results of thermal neutrons in the proposed samples shall be elaborated on at the beginning.

In terms of comparison, the results of thermal neutron beam attenuation through four samples of LBG composites against various thicknesses are illustrated for the two used manners, theoretical and experimental methods, in Figs. 5 and 6. The presented figures emphasize that the attenuation of the thermal neutron flux intensity decreases with the increase of the samples' thicknesses for all samples and for both used techniques.

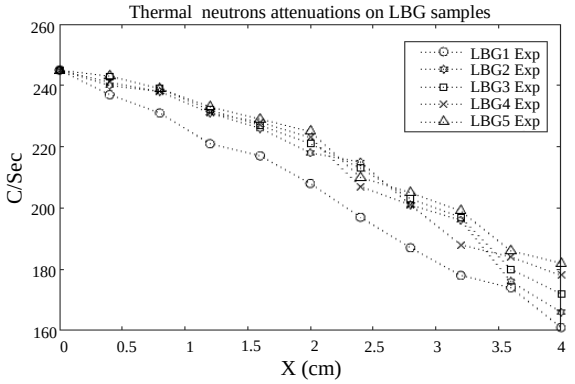


**Fig. 5.** The experimental results of thermal neutron attenuations.

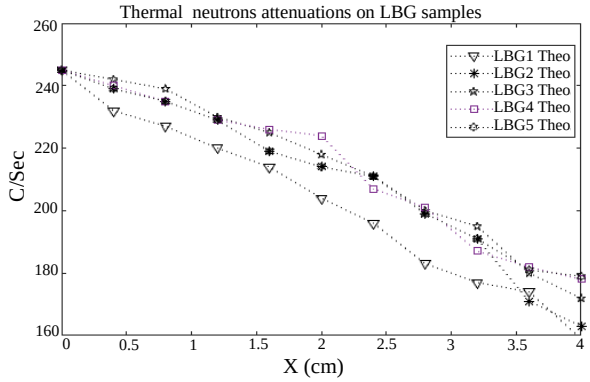


**Fig. 6.** The theoretical results of thermal neutron attenuations.

The attenuations of the flux intensity were studied theoretically, using the Monte Carlo method, versus thicknesses more than the limit that was used in the experimental technique. The yielded results of the MC method are compared statistically in Table 2 using the chi-square value function to investigate the endorsement between our simulation approach and experiments.

**Table 2.** A comparison between the experimental and theoretical (Monte Carlo results of the thermal neutron attenuations through LBG's samples).

| X(cm) | LBG#1 | | LBG#2 | | LBG#3 | | LBG#4 | | LBG#5 | |
|---|---|---|---|---|---|---|---|---|---|---|
| | Exp | Theo | Exp | Theo | Exp | Theo | Exp | Theo | Exp | Theo |
| 0 | 245 | 245 | 245 | 245 | 245 | 245 | 245 | 245 | 245 | 245 |
| 0.4 | 235 | 232 | 240 | 239 | 243 | 242 | 241 | 240 | 243 | 239 |
| 0.8 | 228 | 227 | 238 | 235 | 239 | 239 | 238 | 235 | 239 | 235 |
| 1.2 | 220 | 220 | 231 | 229 | 232 | 230 | 231 | 229 | 233 | 229 |
| 1.6 | 214 | 214 | 226 | 219 | 227 | 225 | 228 | 226 | 229 | 219 |
| 2 | 208 | 204 | 218 | 214 | 221 | 218 | 223 | 224 | 225 | 214 |
| 2.4 | 197 | 196 | 215 | 211 | 213 | 211 | 207 | 207 | 210 | 211 |
| 2.8 | 187 | 183 | 201 | 199 | 203 | 200 | 201 | 201 | 205 | 199 |
| 3.2 | 178 | 177 | 196 | 191 | 197 | 195 | 188 | 187 | 199 | 191 |
| 3.6 | 174 | 174 | 176 | 171 | 180 | 180 | 184 | 182 | 186 | 181 |
| 4 | 161 | 159 | 166 | 163 | 172 | 172 | 178 | 178 | 182 | 179 |
| $\chi^2$ | 0.001956 | | 0.006202 | | 0.00135 | | 0.000927 | | 0.015682 | |

The results of the $\chi 2$ values for all LBG's samples reflect a high endorsement between the theoretical results and experiments and also the reliability of the used theoretical recipe, which relies upon the ingredients of the Monte Carlo method. Besides, the presented results emphasize the capability of all proposed composites of lead borate glazed to attenuate the thermal neutron beams by which it could be used in shielding for facilities of BNCT and also used for filtering against thermal neutrons that are needed in any arbitrary beam shaping assembly system for BNCT based cancer treatment.

According to the illustrated results, it is obvious that the samples which possess a high percentage of boron oxide were favored over the others, and this is intuitively understood due to the high absorption cross-section of boron to thermal neutrons without emitting a high level of gamma-rays.

**Table 3.** Measured total macroscopic cross-section for thermal neutron in different compositions of lead borate glass shields.

| Sample code | ρ ($g.cm^{-3}$) | $\sum_{total}$ ($cm^{-1}$) | HVL(cm) using least square method | HVL(cm) using MC method |
|---|---|---|---|---|
| LBG #1 | 3.95 | 0.10 | 7.01 | 6.95 |
| LBG #2 | 4.37 | 0.09 | 8.09 | 7.99 |
| LBG #3 | 4.89 | 0.07 | 9.55 | 9.46 |
| LBG #4 | 5.01 | 0.06 | 12.49 | 12.3 |
| LBG #5 | 4.41 | 0.05 | 13.70 | 12.5 |
| $\chi 2$ value | | | 0.006089 | |

According to our approach, the total macroscopic cross-sections for thermal neutrons, $\Sigma_t$ in $cm^{-1}$, were recorded for all LBG's samples depending on the investigated attenuations' results displayed in Table 3. It was found that LBG#1 shows the highest $\Sigma_t$ whereas the entire remaining samples exhibit values in the range from 0.05 to 0.09 $cm^{-1}$ by which LBG#1 is considered to be a superior thermal neutron shielding material. Diminution in the total macroscopic cross-sections against thermal neutrons of LBG's samples is associated with the decreases in the percentages of boron and barium in the lead borate glazed samples.

The previous observations emphasize the influence of boron and barium in LBG's samples on thermal neutron absorption which is enhanced by increasing both their percentages in samples and also the samples' thicknesses.

Besides, the half-value layer (HVL) was evaluated for each sample using two techniques, the first was using the least square method to derive the HVL's values from the experimental results, whereas the second was predicting the HVL's values for each sample directly using Monte Carlo simulation method. All these results, as well as densities for each LBG's samples, were illustrated in the same table.

Additionally, the HVL value of LBG#1 was found to be the most applicable value, which increases its implementations in thermal neutron shielding. Moreover, the calculated values of HVL for all samples emphasize that the increasing of boron's percentages in LBG samples decreases the value of HVL at the same percentage of lead.

In our study, the attenuation properties of lead borate glazed materials against gamma rays emitted from different sources of gamma, which use narrow beam geometries, were measured experimentally and computed theoretically using Xcom platform. The attenuation properties, such as the mass attenuation coefficients ($\mu/\rho$), half value layer (HVL), and tenth-value layer (TVL), were studied for each LBG's samples for various thicknesses and illustrated in Figs. 7-11 respectively. Besides, the associated recorded results were represented in Tables 4 and 5 below.

**Table 4.** Measured and calculated mass attenuation coefficient for gamma rays in different compositions of lead borate glass shields.

| LBG # | Mass attenuation coefficient $(\mu/\rho)$ $(cm^2.g^{-1})$ | | | | | | | | | | | |
|---|---|---|---|---|---|---|---|---|---|---|---|---|
| | 356 keV | | 511 keV | | 662 keV | | 1173 keV | | 1274 keV | | 1332 keV | |
| | Exp. | Theo. | Exp. | Theo. | Exp. | Theo. | Exp. | Theo. | Exp. | Theo. | Exp. | Theo. |
| 1 | 0.18910±0.0032 | 0.1910 | 0.1197±0.0027 | 0.1200 | 0.0911±0.0021 | 0.0927 | 0.0599±0.0033 | 0.0597 | 0.0575±0.0054 | 0.0567 | 0.0555±0.0054 | 0.0551 |
| 2 | 0.2112±0.0012 | 0.2003 | 0.1237±0.0047 | 0.1234 | 0.09456±0.0034 | 0.0944 | 0.0598±0.0021 | 0.0600 | 0.0566±0.0036 | 0.0568 | 0.0554±0.0033 | 0.0553 |
| 3 | 0.2250±0.0054 | 0.2190 | 0.1321±0.0043 | 0.1301 | 0.0975±0.0037 | 0.0976 | 0.06123±0.0045 | 0.0604 | 0.0573±0.0065 | 0.0571 | 0.0551±0.0017 | 0.0555 |
| 4 | 0.2045±0.0037 | 0.2026 | 0.1278±0.0034 | 0.1244 | 0.0953±0.0032 | 0.0949 | 0.0612±0.0046 | 0.0601 | 0.0571±0.0054 | 0.0569 | 0.0554±0.0044 | 0.0554 |
| 5 | 0.2198±0.0035 | 0.2091 | 0.1278±0.0065 | 0.1267 | 0.0959±0.0045 | 0.0960 | 0.0600±0.0028 | 0.0602 | 0.0567±0.0056 | 0.0569 | 0.0554±0.0022 | 0.0554 |

**Table 5.** Calculated values of HVL and TVL against gamma rays in different compositions of lead borate glass shields.

| LBG # | Mass attenuation coefficient $(\mu/\rho)$ $(cm^2.g^{-1})$ | | | | | | | | | | | |
|---|---|---|---|---|---|---|---|---|---|---|---|---|
| | 356 keV | | 511 keV | | 662 keV | | 1173 keV | | 1274 keV | | 1332 keV | |
| | HVL | TVL | HVL | TVL | HVL | TVL | HVL | TVL | HVL | TVL | HVL | TVL |
| 1 | 0.918815031 | 3.052554841 | 1.462447257 | 4.858649789 | 1.893135608 | 6.28951429 | 2.939592477 | 9.766130229 | 3.095126471 | 10.2828567 | 3.1850031 | 10.5814514 |
| 2 | 0.791947091 | 2.631064844 | 1.285470035 | 4.27068305 | 1.680370787 | 5.582651359 | 2.643783371 | 8.783371472 | 2.792728914 | 9.278209302 | 2.86848105 | 9.52987863 |
| 3 | 0.64729996 | 2.150507512 | 1.089613307 | 3.61999343 | 1.452445607 | 4.82542157 | 2.346998199 | 7.797369954 | 2.482639075 | 8.248006045 | 2.55421065 | 8.4857864 |
| 4 | 0.682938171 | 2.268907397 | 1.112244963 | 3.695181983 | 1.457990237 | 4.843842347 | 2.302217528 | 7.648596318 | 2.431691976 | 8.078745847 | 2.49753201 | 8.29748445 |
| 5 | 0.751737009 | 2.497475955 | 1.240633059 | 4.121722354 | 1.637377173 | 5.439814815 | 2.611099811 | 8.674787745 | 2.762534422 | 9.177894942 | 2.83733229 | 9.4263939 |

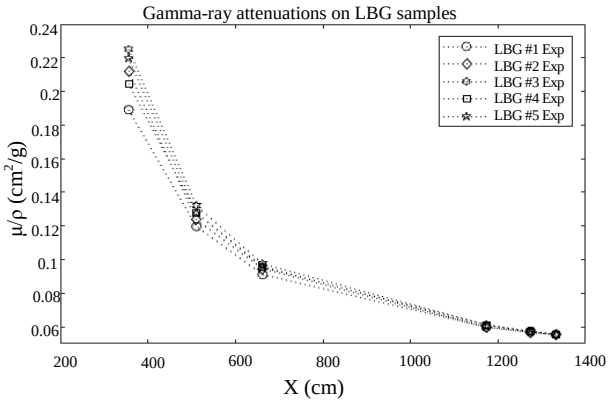


**Fig. 7.** Dependence of experimental mass attenuations coefficients on photon energies transmitted through LBG samples.

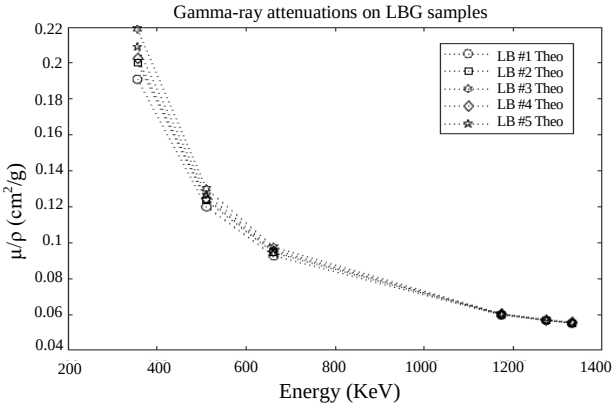


**Fig. 8.** Dependence of theoretical mass attenuations coefficients on photon energies transmitted through LBG samples.

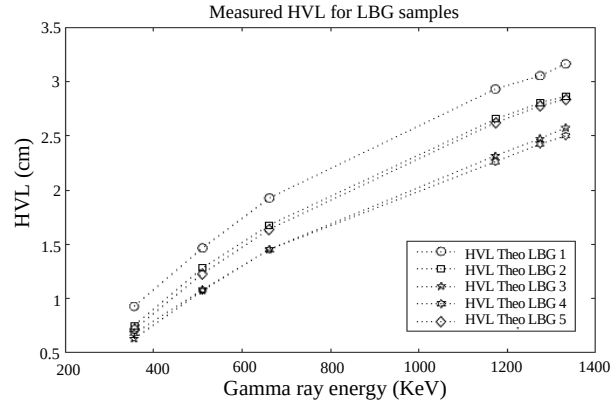


**Fig. 9.** Measured HVL for LBG samples at different photon energies.

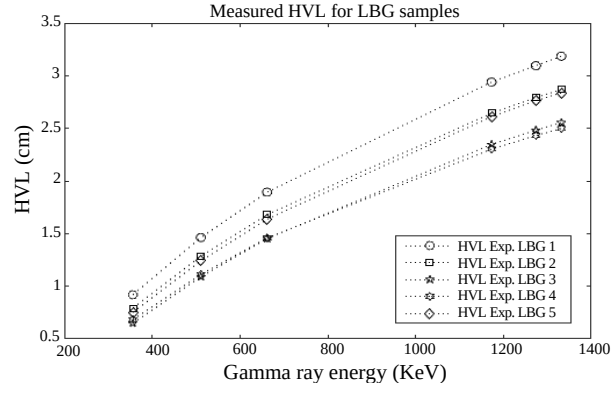


**Fig. 10.** Theoretical HVL for LBG samples at different photon energies using MC.

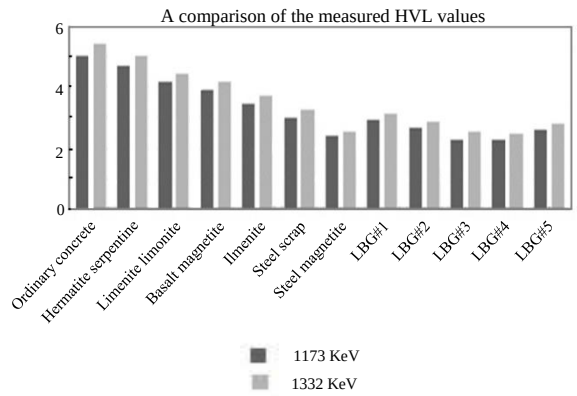


**Fig. 11.** The measures values of HVL for LBG samples and other shielding materials from the previous studies.

According to the obtained results of the mass attenuation coefficients of LBG samples, all the proposed LBG composites exhibited appropriate attenuation values which emphasize the applicability of our composites for shielding applications against gamma-rays for medical applications, particularly in radiotherapy. Although specific energies of gamma-ray have been used in our investigations, it was observed that the μ/ρ values are high in the region of the photoelectric absorption and reduce gradually with increasing the energies of emitted gamma to be the lowest nearing the Compton-scattering region.

Moreover, the curves of μ/ρ versus the photon energy emphasize the associated mass attenuations of LBG samples are optimized by increasing the percentages of the additive oxides. Intuitively, the measured μ/ρ values decrease by increasing the energies of the incident gamma beams.

Additionally, to emphasize the capability of our proposed materials for shielding purposes against gamma-ray in various radiotherapy facilities, the yielded results of LBG's samples were compared with the results obtained by previous studies for other materials at energies 1173 and 1332 keV of gamma-rays emitted by Co-60 gamma source. The compared results are represented in Table 6.

**Table 6.** Comparison of gamma-ray shielding capability of the investigation composited with studied shielding materials.

| Shielding materials | | ρ, (g·cm$^{-3}$) | 1173 keV | 1332 keV |
|---|---|---|---|---|
| | | | MAC*, cm$^{-2}$·g$^{-1}$) | MAC*,cm$^{-2}$·g$^{-1}$) |
| [17] | Ordinaryconcrete | 2.30 | 0.0594 | 0.0556 |
| | Hematiteserpentine | 2.50 | 0.0585 | 0.0548 |
| | Ilmenitelimonite | 2.90 | 0.0572 | 0.0536 |
| | Basaltmagnetite | 3.05 | 0.0583 | 0.0546 |
| | Ilmenite | 3.50 | 0.0571 | 0.0535 |
| | Steel Scrap | 4.00 | 0.0571 | 0.0535 |
| | Steelmagnetite | 5.11 | 0.0565 | 0.0529 |
| THIS WORK | LBG #1 | 3.95 | 0.0599 | 0.0555 |
| | LBG #2 | 4.37 | 0.0598 | 0.0554 |
| | LBG #3 | 4.89 | 0.0612 | 0.0551 |
| | LBG #4 | 5.01 | 0.0612 | 0.0554 |
| | LBG #5 | 4.41 | 0.0600 | 0.0554 |

In terms of comparisons, the values of the mass attenuation coefficients of LBG samples were so close to these values of the previous studies which prove the capability of the proposed LBG composites for shielding against gamma-rays at these energies. Moreover, our proposed materials possess additive satisfactory features such as affordability, availability, stability against various environmental operating positions, transparency, and ultimately the waterproof ability.

The measured values of HVL for LBG samples and other shielding materials from the previous studies have been compared and illustrated in Fig. 11. According to the represented results in Fig. 11, the values of HVL of the LBG samples and steel magnetite were found to be preferred over values that are associated with other materials which emphasizes the reliability and capability of the proposed LBG composites for shielding purposes of BNCT and other radiotherapy facilities.

Ultimately, it is suggested to investigate other samples of LBG with higher proportions of boron to find the optimum value for the boron percentage without affecting the mechanical properties of those samples. It is also recommended to make an extension of these measurements by adding elements other than lead such as tungsten or titanium to be used as a sufficient barrier to gamma rays and thermal neutrons without secondary hard gamma rays. It is also recommended to conduct other tests on materials with high efficiency to attenuate radiation, such as ceramics and polymers with different proportions of boron or barium with a high cross-sectional area with thermal neutrons. Besides, it also is recommended to test multilayer combinations of steel, graphite and polyethylene for use as a filter for fast neutrons by shifting their energies into the thermal neutrons region.

## CONCLUSION

Five composites of lead borate glazed materials have been studied for shielding purposes for BNCT units and other radiotherapy applications. The composites were shielding thermal neutrons emitted by the Cf-252 neutron source. Our results show effective shielding of lead borate materials with small HVL values for high lead and boron composites. Experimental measurements of the simulation results emphasize the validation of the implemented mathematical models. The filtering capabilities of LBG composites, for gamma-rays, of energy-spectra have been investigated and compared with other published materials at 1173 and 1332 KeV energies. Our LBG samples, with optimized lead and boron percentages, specifically LBG#1, show superior shielding properties over previously suggested shielding materials referenced in this work.

## ACKNOWLEDGMENT

Initially, M. S. Ali would like to acknowledge the AIMS-Senegal committee for their continued support. Additionally, M. S. Ali would like to acknowledge Prof. Dr. M. Ahmed, the assistant professor, at Vanderbilt University, United States. He always finds the time to quell my confusion, and I wish him all the best with his future scientific projects. The authors are grateful to the anonymous referee for careful checking of the details and for helpful comments that improved this paper.

## AUTHOR CONTRIBUTION

M. S. Ali and A. M. Abdelmonem equally contributed as the main contributors to this paper. G. S. Hassan contributed a substantial intellectual contribution and supervised the work. All authors read and approved the final version of the paper.

## REFERENCES

1. W. A. G. Sauerwein, A. Wittig, R. Moss *et al.*, Neutron Capture Therapy Principles and Applications, Springer Heidelberg, New York (2012) 1.
2. S. Shalbi, N. Sazali and W. N. W. Salleh, IOP Conf. Ser.: Mater. Sci. Eng. **736** (2020) 062021.
3. J. Burian, S. Flibor, M. Marek *et al.*, J. Phys. Conf. Ser. **41** (2006) 174.
4. K. Nedunchezhian, N. Aswath, M. Thiruppathy *et al.*, J. Clin. Diagn. Res. **10** (2016) ZE01.
5. C. J. Gohil and M. N. Noolvi, Int. J. Pharm. Chem. Anal. **2** (2015) 192.
6. I. Ardana and Y. Sardjono, Tri Dasa Mega **19** (2017) 121. (in Indonesian)
7. R. S. Kaundal, Mater. Res. **19** (2016) 776.
8. K. J. Singh, N. Singh, R. S. Kaundal *et al.*, Nucl. Instrum. Methods Phys. Res., Sect. B **266** (2008) 944.
9. V. P. Singh and N. M. Badiger, Phys. Res. Int. **2014** (2014) 1.

10. S. Glasstone and A. Sesonske, Nuclear Reactor Engineering: Reactor Systems Engineering, 4th ed., Springer Science & Business Media (2012) 1.

11. J. K. Shultis and R. E. Faw, Health Phys. Soc. **88** (2005) 587.

12. IAEA, *Terminology Used in Nuclear Safety and Radiation Protection*, in: IAEA Safety Glossary, 2007 Edition, International Atomic Energy Agency, Vienna (2007) 1.

13. J. E. Martin, Physics for Radiation Protection, 3rd ed., Wiley-VCH Verlag & Co. KGaA, Weinheim (2013) 1.

14. J. K. Shultis and R. E. Faw, Errata for Radiation Shielding, Prentice-Hall, New Jersey (1996) 1.

15. M. K. Narayanan and H. D. Shashikala, Procedia Mater. Sci. **5** (2014) 303.

16. F. S. Abdo, W. A. Kansouh, A. Kelany *et al.*, Arab J. Nucl. Sci. Appl. **43** (2010) 103.

17. I. I. Bashter, Ann. Nucl. Energy **24** (1997) 1389.